Geophys. J. Int. (2002) **149,** 534–545

Reduction of surface gravity data from global atmospheric pressure loading

Jean-Paul Boy,[1,2] Pascal Gegout[1] and Jacques Hinderer[1]

[1] *EOST-IPGS (UMR* 7516 *CNRS-ULP),* 5 *rue Rene Descartes,* 67084 *Strasbourg Cedex, France*
[2] *Space Geodesy Branch, Code* 926, *NASA's Goddard Space Flight Center, Greenbelt, MD* 20771, *USA*

Accepted 2001 December 6. Received 2001 December 6; in original form 2001 March 12

SUMMARY

Besides solid Earth and ocean tides, atmospheric pressure variations are one of the major sources of surface gravity perturbations. As shown by previous studies (Merriam 1992; Mukai *et al.* 1995; Boy *et al.* 1998), the usual pressure correction with the help of local pressure measurements and the barometric admittance (a simple transfer function between pressure and gravity, both measured locally) does not allow an adequate estimation of global atmospheric loading. We express the response of the Earth to pressure forcing using a Green's function formalism (Farrell 1972). The atmosphere acts on surface gravity through two effects: first, a direct gravitational attraction by air masses which is sensitive to regional (about 1000 km around the gravimeter) pressure variations; second, an elastic process induced by the Earth's surface deformation and mass redistribution which is sensitive to large scale pressure variations (wavelengths greater than 4000 km).

We estimate atmospheric loading using Green's functions and global pressure charts provided by meteorological centres. We introduce different hypotheses on the atmospheric thickness and atmospheric density variations with altitude for the modelling of the direct Newtonian attraction. All computations are compared to gravity data provided by superconducting gravimeters of the GGP (Global Geodynamics Project) network. We show the improvement by modelling global pressure versus the local estimates in terms of reduction of the variance of gravity residuals. We can also validate the inverted barometer (IB) hypothesis as the oceanic response to pressure forcing for periods exceeding one week. The non-inverted barometer (NIB) hypothesis is shown to be definitely an inadequate assumption for describing the oceanic response to atmospheric pressure at seasonal timescales.

Key words: atmospheric loading, Green's function, pressure, superconducting gravimeter.

1 INTRODUCTION

Superconducting gravimeters are a privileged tool to study the Earth's global and internal dynamics (see for example Crossley *et al.* 1999) over a large period range (from a few minutes to several years). However the atmosphere is, after solid Earth tides, one of the major sources of perturbations of surface gravity and masks small contributions such as core modes or anelastic effects on tides.

Atmospheric loading effects are usually corrected using an empirical estimation, called barometric admittance (Warburton & Goodkind 1977; Crossley *et al.* 1995), which is a simple transfer function adjusted by least square fitting between pressure and gravity, both measured locally. In fact, however, the global atmosphere acts on surface gravity through two effects: a direct Newtonian attraction by air masses and an elastic contribution due to the Earth's surface displacement and mass redistribution (e.g. Spratt 1982; Mukai *et al.* 1995; Boy *et al.* 1998). The simple correction using only the local pressure measurement cannot take into account the large scale pressure structures existing over the whole surface of the Earth, and is therefore not sufficient to estimate either the induced global deformation and mass redistribution of the Earth or the Newtonian direct attraction induced by regional (1000 km around the gravimeter) mass variations.

The purpose of this paper is to estimate surface gravity variations induced by the atmospheric circulation with a physical approach and to propose an operational modelling using global atmospheric data provided by meteorological centres. As a first step, we determine and describe the physics of the source (the atmosphere) and the transfer functions (Newtonian and elastic atmospheric Green's functions). For the computation of the gravitational attraction, we consider different models for the atmosphere. We then describe the superconducting gravimeter observations and their processing. The next section is devoted to the determination of the optimal model for computing the atmospheric loading; special attention is paid to the ocean response to pressure.

2 GLOBAL ATMOSPHERIC CIRCULATION

In this section, we present the two atmospheric data sets that we will use to estimate global atmospheric loading. We show that pressure variations are characterized by large scale structures with wavelengths greater then 4000 km. We recall that the hydrostatic equilibrium hypothesis is verified for periods larger than 12 hr (Green 1999), so the estimation of atmospheric density variations with altitude, as a function of surface pressure and temperature conditions with the help of the hydrostatic equilibrium equation, is adequate for our atmospheric data.

2.1 Atmospheric data

We use global meteorological data sets provided by the U.S. National Center for Environmental Prediction (NCEP) and the European Centre for Medium-range Weather Forecasts (ECMWF).

The first data set, provided by the NCEP, consists of surface pressure data with a sampling rate of 6 hr and a spatial resolution of 2.5° in latitude and longitude. These NCEP reanalysis data are provided using a state-of-the-art analysis system to perform data assimilation from 1948 to the present.

The second surface data set, provided by the ECMWF, covers the period 1985–1996. The time sampling rate is the same as the NCEP reanalysis series (6 hr). The spatial sampling is 1.125° for latitude and longitude.

2.2 Spectral energy

The spectral energy per degree represents the energy of pressure variations as a function of the harmonic degree n,

$$R(n,t) = \sum_{m=0}^{n} \left\{ \left[p_n^m(t)\right]^2 + \left[\tilde{p}_n^m(t)\right]^2 \right\}, \quad (1)$$

where $p_n^m(t)$ and $\tilde{p}_n^m(t)$ are the cosine and sine terms of degree n and order m in a spherical harmonic decomposition of the time dependent surface pressure field.

In a spherical harmonic decomposition, the wavelength $\lambda(n)$ can be associated to the harmonic degree n,

$$\lambda(n) = 2\pi \frac{a}{n}, \quad (2)$$

where a is the mean radius of the Earth.

Fig. 1 shows the spectral energy of the surface pressure field provided by ECMWF for the year 1994. Pressure variations are dominated by very low harmonic degrees, typically $n < 10$, corresponding to large scale atmospheric structures ($\lambda > 4000$ km).

Degrees 1 and 3 which include S_1 and Sa (diurnal and annual thermal waves) are shown to be variable in time with a seasonal component.

For periods exceeding a few hours, the atmospheric circulation is principally governed by horizontal displacements (Green 1999). The hydrostatic equilibrium is verified and we can use the corresponding equation to estimate density variations with altitude as a function of surface parameters (temperature and pressure).

There is also a relationship between the horizontal wavelength and the period of atmospheric variations (Green 1999). High frequency pressure variations are coherent on small scale surfaces whereas low frequency atmospheric structures are coherent on large scale surfaces. For example, mid-latitude circulation (anticyclonic-depression) has typical periods of about 5–10 days and wavelengths of several thousands of kilometres.

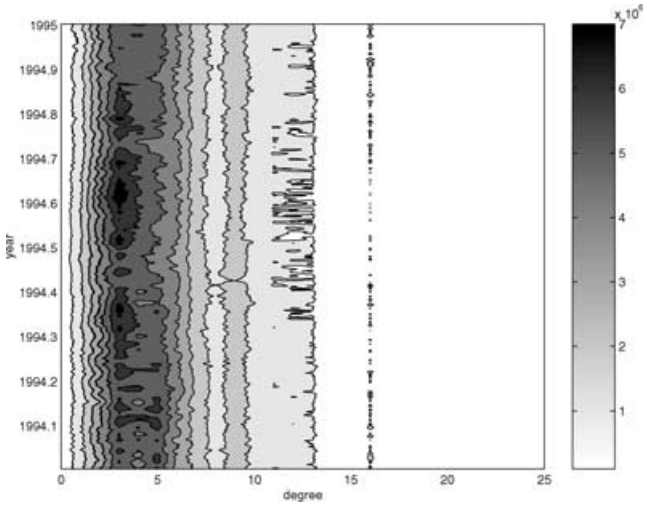

Figure 1. Spectral energy of surface pressure field (ECMWF) in Pa^2 as a function of spherical harmonic degree n and for the year 1994.

3 ATMOSPHERIC GREEN'S FUNCTIONS

As shown by previous studies (e.g. Spratt 1982; Mukai *et al.* 1995; Boy *et al.* 1998), the global atmosphere acts on surface gravity through two effects:

(1) a direct gravitational attraction by air masses
(2) an elastic contribution from the Earth's surface deformation and self-potential variations due to loading boundary conditions at the Earth's surface.

We determine hereafter the Earth response to atmospheric loading in terms of surface gravity variations in the spatial domain using a Green's function formalism. We first introduce different models for the atmosphere used in the computation of the Newtonian attraction effect, then we discuss the modelling of the elastic contribution.

3.1 Direct Newtonian attraction

In this section devoted to the Newtonian attraction caused by atmospheric masses, we introduce different models for the atmosphere. The most complete one is the 3-D model where pressure, temperature and humidity are changing with latitude, longitude and altitude. We keep the thin-layer model as the classical simple model used for treating atmospheric loading following Farrell's (1972) approach. We then derive our preferred pseudo-stratified model from the 3-D model using reasonable approximations and we show that the gravity changes can then be obtained from the convolution of the Green's function with surface pressure data.

3.1.1 3-D atmosphere

The Newtonian effect corresponds to a direct gravitational attraction by air masses on the gravimeter. Following Merriam (1992), we define

$$GS(\psi, z) = \frac{G[a - (a+z)\cos\psi]}{[a^2 + (a+z)^2 - 2a(a+z)\cos\psi]^{(3/2)}}, \quad (3)$$

where z is the altitude of the atmospheric elementary volume of density ρ_A and spherical coordinates (θ', λ') and G is the Newtonian constant of gravitation. ψ is the angular distance between the gravimeter of coordinates (θ, λ) and the elementary atmospheric mass. That angular distance can be expressed as a function of both coordinates,

$$\cos\psi = \cos\theta\cos\theta' + \sin\theta\sin\theta'\cos(\lambda - \lambda') \tag{4}$$

The Newtonian attraction of the surface gravity variations in (θ, λ) are in the case of a stratified atmosphere, of finite thickness (20 km) and with variations of pressure, temperature and humidity with height,

$$\delta g_{\text{Newtonian}}(\theta, \lambda, t) = \iiint GS(\psi, z')\rho_A(\theta', \lambda', z', t)\, dv'. \tag{5}$$

In this general case, the 3-D integration over the whole atmosphere needs to estimate the atmospheric density everywhere to compute the direct Newtonian attraction of the atmosphere. Global atmospheric data provided by meteorological centres consist of pressure, temperature and specific humidity data at different vertical levels. We have to use these data to rebuild atmospheric density variations.

The atmosphere is classically treated as a mixture of dry air and water vapor. The ideal gas equation gives us relations between temperature T, density ρ_A and pressure p for both components (Gill 1982),

$$\begin{aligned} p_d &= \rho_d R T \\ p_v &= \rho_v R_v T \end{aligned}, \tag{6}$$

where p_d and ρ_d are respectively the partial pressure and the density of dry air. p_v and ρ_v are the partial pressure and the density of water vapor. R_v and R are respectively the universal gas constant for water vapor and for dry air and are respectively equal to 461.50 J kg^{-1} K^{-1} and 287.04 J kg^{-1} K^{-1}.

For a gas mixture, the total pressure p is the sum of all partial pressures,

$$p = p_d + p_v. \tag{7}$$

We note q, the specific humidity, the ratio between density of water vapor and the density of gas mixture and is given by

$$q = \frac{\rho_v}{\rho_A} = \frac{\rho_v}{\rho_d + \rho_v}. \tag{8}$$

The total density ρ_A becomes

$$\rho_A = \frac{p}{RT\left(1 - q + \dfrac{q}{\epsilon}\right)}, \tag{9}$$

where ϵ is equal to

$$\epsilon = \frac{R}{R_v} = 0.62197. \tag{10}$$

We use the classical virtual temperature, noted T_v,

$$T_v = T\left(1 - q + \frac{q}{\epsilon}\right). \tag{11}$$

The density of the atmosphere becomes

$$\rho_A = \frac{p}{RT_v} = \frac{p}{RT\left(1 - q + \dfrac{q}{\epsilon}\right)}. \tag{12}$$

This model requires a convolution of the Green's function $GS(\psi, z)$ with the 3-D atmospheric density (eq. 12) for the whole atmosphere. This computation requires large computing resources. However, as described below, there is a way to approximate the estimation of the direct attraction of air masses on the gravimeter by simplifying the 3-D convolution into a 2-D convolution using only surface atmospheric data.

3.1.2 Thin-layer model

As a first approximation, we can classically neglect the atmospheric thickness. In this case, the surface atmospheric density $\sigma_A(\theta', \lambda')$ is directly linked to the surface pressure variation $p_0(\theta', \lambda')$,

$$p_0(\theta', \lambda') = \sigma_A(\theta', \lambda')g_0, \tag{13}$$

where g_0 is the mean surface gravity. This value is taken constant and we neglect the small changes due to the latitude dependence, which are not taken into account by the meteorological models in any case.

In this model we define the Newtonian Green's function by (Farrell 1972)

$$GN(\psi) = -\frac{G}{g_0 a^2}\sum_{n=0}^{+\infty} n P_n(\cos\psi), \tag{14}$$

where P_n is the Legendre polynomial of degree n. Notice that this Green's function does not have the same dimension as GS in eq. (3). The series expansion can be written as (Farrell 1972)

$$GN(\psi) = \frac{G}{g_0 a^2}\left[\frac{1}{4\sin(\psi/2)} - 2\pi a^2\delta(\psi)\right] \tag{15}$$

where $\delta(\psi)$ is the Dirac function and represents the contribution of the mass just above the gravimeter and is equal to the Bouguer semi-infinite plate value (-4.27 nm s^{-2} hPa^{-1}).

For a more detailed derivation of these results, the reader may refer to previous studies (e.g. Spratt 1982; Boy *et al.* 1998).

In this case, the surface gravity variations in (θ, λ) induced by direct Newtonian attraction are equal to

$$\delta g_{\text{Newtonian}}(\theta, \lambda, t) = \iint_{\text{surface}} GN(\psi)p_0(\theta', \lambda', t)\, ds', \tag{16}$$

where $ds' = a^2\sin\theta'\, d\theta'\, d\lambda'$ is the surface element of integration.

This approximation allows a drastic reduction of the computing time because the Newtonian Green's function is only convolved with the surface pressure field. However, this model does not take into account the curvature of the atmosphere, in particular the relative position of the atmospheric masses being above or under the local horizon (Merriam 1992).

3.1.3 Pseudo-stratified model

The second approximation does not neglect the atmospheric thickness but approximates density variations with altitude as only depending on surface pressure and temperature.

For periods exceeding a few hours, i.e. the temporal sampling of global meteorological data, the atmospheric circulation is principally governed by horizontal displacements (e.g. Green 1999). Hydrostatic equilibrium is then a valid approximation and gives pressure variations dp as a function of altitude variations dz,

$$dp = -\rho_A g_0\, dz. \tag{17}$$

If we consider the atmosphere as a perfect gas, the state law gives the relation between pressure p, density ρ_A and temperature T,

$$p = \rho_A RT. \tag{18}$$

The decrease of temperature with altitude can be modelled as a linear trend,

$$T(z) = T_0 + \alpha z. \tag{19}$$

$\alpha = -6.49$ K km^{-1} in the case of the Standard Atmosphere (NOAA/NASA/USAF 1976).

We neglect in this case the influence of water vapor content. In fact, it is very small compared to the temperature influence and is impossible to model using a simple law (linear, exponential...).

By combining the last three equations, we can write the variations of density $d\rho_A(z)$ as a function of altitude variations dz,

$$\frac{d\rho_A(z)}{\rho_A(z)} = -\frac{g_0}{R}\frac{dz}{T_0 + \alpha z}\left(1 + \frac{R\alpha}{g_0}\right). \tag{20}$$

The integration of this equation leads to the expression of the density as a function of the altitude and surface conditions (temperature T_0 and pressure P_0)

$$\rho_A(z) = \frac{P_0}{RT(z)}\left(1 + \frac{\alpha}{T_0}z\right)^{-g_0/R\alpha}. \tag{21}$$

The law expressing the pressure variations is very similar,

$$P(z) = P_0\left(1 + \frac{\alpha}{T_0}z\right)^{-g_0/R\alpha}. \tag{22}$$

For an isothermal atmosphere ($T(z) = T_0$ or $\alpha = 0$), the variations of density and pressure with the altitude z follow from eq. (20) and are equal to

$$\rho_A(z) = \frac{P_0}{RT_0}\exp\left(-\frac{g_0 z}{RT_0}\right) \tag{23}$$

$$P(z) = P_0 \exp\left(-\frac{g_0 z}{RT_0}\right) \tag{24}$$

Fig. 2 shows the differences in pressure, temperature and density between the US Standard Atmosphere (NOAA/NASA/USAF 1976), the hydrostatic approximation with a linear decrease of temperature with altitude (eqs 21 and 22) and the hydrostatic approximation with a constant temperature (isothermal) (eqs 23 and 24).

In Fig. 2, the pressure and temperature conditions at the surface in the hydrostatic models are the same as for the standard atmosphere model. For an altitude smaller than 12 km, the temperature profile in the hydrostatic approximation with linear temperature decrease is equivalent to the one corresponding to the standard atmosphere.

However Fig. 2 also shows that the isothermal approximation does not change significantly the density profile. We hence use these assumptions (isothermal and hydrostatic) to compute the direct Newtonian attraction of air masses and call it the pseudo-stratified model.

This simple model of atmosphere using pressure and temperature at the Earth's surface allows us a good estimation of density variations with altitude up to 20 km which is the upper limit used in this study.

In this case, we can introduce a pseudo-stratified Newtonian Green's function $GS_{PS}(\psi)$,

$$GS_{PS}(\psi) = \int_{z=0}^{20\,\mathrm{km}}\left[GS(\psi, z)\frac{1}{RT_0}\exp\left(-\frac{g_0 z}{RT_0}\right)\right]dz, \tag{25}$$

where $GS(\psi, z)$ is the Newtonian Green's function for a stratified atmospheric model.

The gravity changes in (θ, λ) are only a function of surface pressure conditions and become

$$\delta g_{\mathrm{Newtonian}}(\theta, \lambda, t) = \iint_{\mathrm{surface}} GS_{PS}(\psi)p_0(\theta', \lambda', t)\,ds'. \tag{26}$$

We neglect the temperature variations in time and space as they lead to smaller effects than the pressure-induced ones, of the order of a few per cent as shown by Merriam (1992).

This equation is very similar to the one obtained for the thin-layer model (eq. 16) and allows us to decrease the computing time by simplifying the 3-D convolution for the real atmosphere into a 2-D convolution.

3.2 Elastic contribution

The elastic contribution in gravity originates from the surface deformation (vertical motion in the Earth's gravity field) and from the Earth's mass redistribution (altering the gravitational potential) and is usually expressed in the spectral domain, i.e. using a spherical harmonic approach (Sneeuw & Bun 1996), with dimensionless Love numbers, i.e. non-dimensional factors between the source (here a loading process) and the consequences (displacement, potential).

We assume that the elastic contribution is induced here by a surface loading process (thin-layer approximation for the atmosphere) even though we model the gravitational attraction using a stratified loading process. We can use the load Love numbers h'_n and k'_n which are respectively the load radial and potential Love numbers (Hinderer & Legros 1989). These numbers are computed in this study from the Preliminary Reference Earth Model (PREM) (Dziewonski & Anderson 1981).

The elastic Green's function is equal to (e.g. Farrell 1972; Spratt 1982; Boy *et al.* 1998),

$$GE(\psi) = -\frac{G}{g_0 a^2}\sum_{n=0}^{+\infty}[2h'_n - (n+1)k'_n]P_n(\cos\psi). \tag{27}$$

The elastic contribution to the gravity changes at (θ, λ) is equal to

$$\delta g_{\mathrm{Elastic}}(\theta, \lambda, t) = \iint_{\mathrm{surface}} GE(\psi)p_0(\theta', \lambda', t)\,ds'. \tag{28}$$

Numerical estimates of Green's functions require the computation of Love numbers up to a high spherical harmonic degree ($n = 9000$ in this study). Numerical integration of the elasto-gravitational equations provide a set of independent solutions in each layer. The fluid core in hydrostatic equilibrium is governed by a set of only two differential equations. Solving the set of boundary conditions at each interface and at the surface provides the Love numbers. Love numbers for high degrees ($n > 250$) are obtained by considering that surface loading produces no deformation within the liquid core and the solid inner core, i.e. a new set of boundary conditions on the mantle is defined with no deformations at the CMB (core-mantle boundary) and boundary conditions at the Earth's surface. We also took into account in the spherical harmonic expansion the degree-one Love numbers (Greff-Lefftz & Legros 1997) which are expressed here in the centre-of-mass reference frame. We do not take into account the Earth's deformation of degree $n = 0$. However, as we subtract the mean pressure field to the surface pressure data, the degree $n = 0$ contribution can be neglected.

The surface gravity variations due to a surface loading can be expressed in the spectral domain, i.e. in a spherical harmonic approach as follows (Spratt 1982; Hinderer & Legros 1989):

$$\delta g(\theta, \lambda, t) = \sum_{n=0}^{+\infty}\sum_{m=0}^{n}\left(-\frac{3}{2n+1}\frac{n\delta'_n}{a\rho}\right)p_n^m(t)Y_n^m(\theta, \lambda), \tag{29}$$

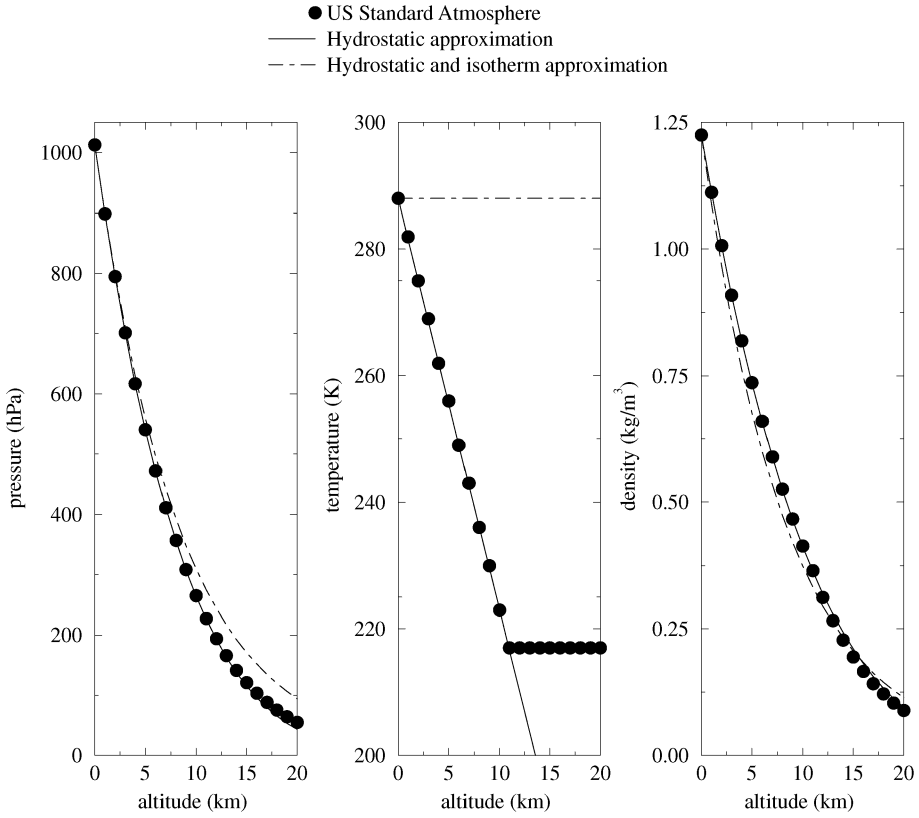

Figure 2. Pressure, temperature and density variations with altitude for the US Standard Atmosphere (NOAA/NASA/USAF 1976), the hydrostatic (linear decrease of temperature with altitude) and the hydrostatic and isothermal approximations.

where $p_n^m(t)$ are the spherical harmonic coefficients of the time dependent surface pressure field and $Y_n^m(\theta, \lambda)$ are the spherical harmonic functions. ρ is the mean density of the Earth. δ'_n is the gravimetric factor of degree n and is equal to (Hinderer & Legros 1989)

$$\delta'_n = 1 + \frac{2}{n} h'_n - \frac{n+1}{n} k'_n. \tag{30}$$

Fig. 3 shows the spectral response of the Earth, in terms of surface gravity changes, to a thin-layer surface loading for the elastic contribution (the term $\frac{2}{n}h'_n - \frac{n+1}{n}k'_n$ in eq. 30), and for the direct Newtonian attraction (the term 1 in eq. 30). These effects are characterized by opposite physical processes. The elastic contribution appears to be induced by large scale pressure coherence (or low harmonic degrees), typically of wavelengths greater than 4000 km ($n<10$), whereas the direct Newtonian attraction acts with the opposite sign and is induced by regional (distances smaller than 1000 km) pressure variations around the gravimeter.

We finally propose two hypotheses for the estimation of the direct Newtonian attraction: a thin-layer surface approximation which neglects the atmospheric thickness, and a pseudo-stratified isothermal model which approximates density variations with altitude using the hydrostatic equilibrium equation. The elastic contribution, which has an amplitude roughly ten times smaller than the direct attraction, is modelled using a thin-layer surface loading hypothesis. For both cases, the gravity variations in (θ, λ) are only functions of surface pressure conditions $p_0(\theta', \lambda', t)$ and are equal to

$$\delta g(\theta, \lambda, t) = \iint_{\text{Surf}} (GE(\psi) + GN(\psi))\, p_0(\theta', \lambda', t)\, ds', \tag{31}$$

for the thin-layer approximation, and

$$\delta g(\theta, \lambda, t) = \iint_{\text{Surf}} (GE(\psi) + GS_{PS}(\psi))\, p_0(\theta', \lambda', t)\, ds' \tag{32}$$

for the pseudo-stratified hypothesis.

Fig. 4 shows the elastic and the Newtonian Green's functions, i.e. the spatial response of the Earth to a pseudo-stratified atmospheric loading model as a function of angular distance ψ. The non-regular shape (slope change) appearing in the elastic Green's function for

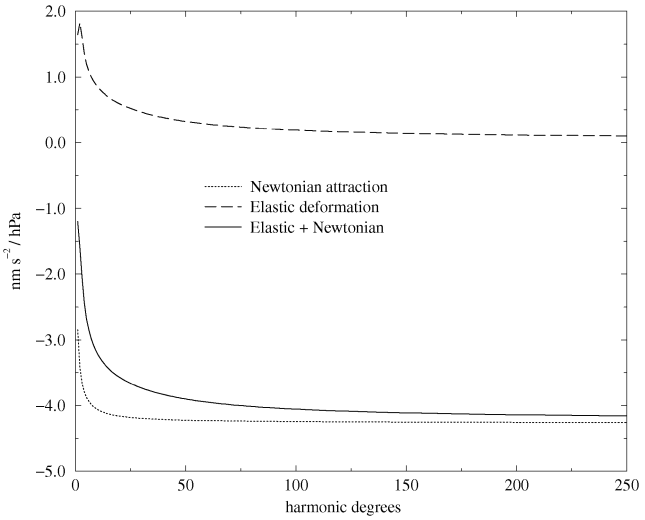

Figure 3. Spectral Earth response (elastic contribution and Newtonian attraction) to a surface pressure loading in terms of surface gravity changes as a function of spherical harmonic degree n.

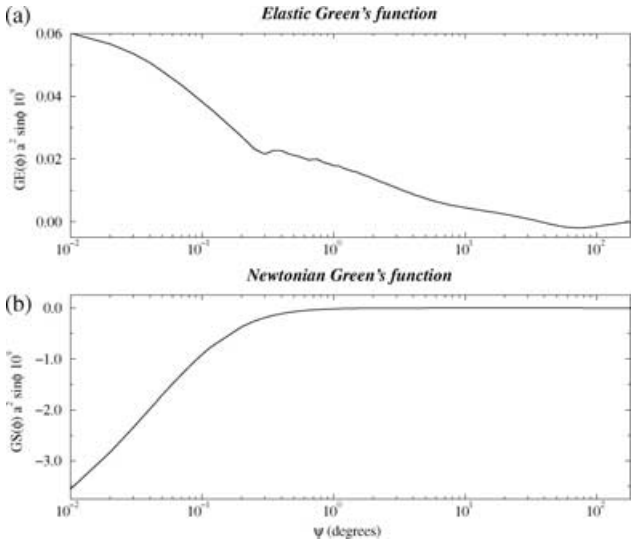

Figure 4. Spatial Earth response to pressure loading (a) elastic contribution and (b) pseudo-stratified Newtonian attraction.

specific angular distances (between 0.2 and 0.7°) is related to the evolution of the Love numbers as a function of the harmonic degree, n, (see e.g. Boy 2000, Fig. I.1). This is probably linked to some major discontinuities in the elastic parameters in the Earth.

4 SUPERCONDUCTING GRAVIMETER OBSERVATIONS AND METHODOLOGY

The surface gravity residuals are the observed gravity corrected for the following principal effects:

(1) the instrumental drift modelled by a linear or an exponential function;

(2) the Earth's rotation induced effects (length-of-day variations and polar motion);

(3) solid and oceanic tides adjusted by least-squares fitting using the tidal analysis software ETERNA 3.30 (Wenzel 1996); and

(4) an atmospheric correction, either the local barometric admittance adjustment or the subtraction of the global atmospheric loading estimated with the help of the Green's functions previously calculated and global pressure charts provided by ECMWF or NCEP.

Our purpose is to assess whether the modelling of global atmospheric loading produces a significant and systematic reduction of the variance of surface gravity residuals using different superconducting gravimeters from the GGP (Global Geodynamics Project) network (Crossley *et al.* 1999) with the global atmospheric loading estimates versus the usual local pressure correction.

We explain the preprocessing of raw minute gravity and pressure data provided by GGP and the modelling of the Earth's rotation induced effects. We also discuss the practical computation of global atmospheric loading.

4.1 Data preprocessing

Among the twenty superconducting gravimeters of the GGP network, we analyze data provided by six instruments: Boulder (BO) in Colorado, Canberra (CB) in Australia, Esashi (ES) in Japan, Membach (MB) in Belgium, Strasbourg (ST) in France and Vienna (VI) in Austria; their locations are shown in Fig. 5. We chose these six stations because of their locations. Canberra and Esashi are close to the Pacific Ocean, whereas Boulder is far from the Atlantic and Pacific Ocean. Membach, Strasbourg and Vienna are located at increasing distances from the North Sea and the North Atlantic in western Europe.

This network delivers raw gravity and pressure data at a sampling rate of one minute. Raw gravity and pressure data are first corrected for major perturbations on a few samples such as offsets, gaps and spikes by substituting a synthetic local tide (Crossley *et al.* 1993). Data are then filtered to a sampling of 6 hr corresponding to the sampling rate of global pressure charts.

The effects induced by the Earth's rotation variations (polar motion and length-of-day) are then subtracted, assuming a static polar tide in the oceans. The gravimetric factor δ_2 becomes equal to 1.18 (1.16 for the solid Earth only) for the amplitude and 0° for the phase (Loyer *et al.* 1999; Boy 2000). This assumption is generally a good approximation of the oceanic response to Earth's rotation variations, except for some specific areas like the North and Baltic Seas (Xie & Dickman 1995). However notice that we do not model other environmental contributions such as oceanic circulation, water table or soil moisture which can lead, in some cases, to effects reaching several tens of nm s^{-2} (Van Dam & Wahr 1998), i.e. larger than the effect induced by the dynamics of the pole tide in the North and Baltic Seas.

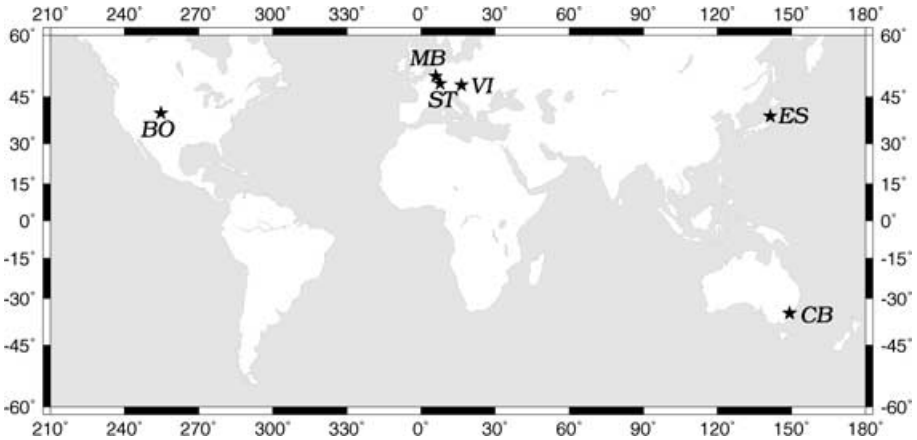

Figure 5. Location of the six gravimeters of GGP network whose data are analyzed in this paper.

The gravity changes in (θ, λ) are equal to (e.g. Loyer *et al.* 1999)

$$\delta g_{rot}(\theta, \lambda, t) = \tilde{\delta}_2 \Omega^2 a \left[2m_3 \sin^2\theta - \sin 2\theta (m_1 \cos\lambda + m_2 \sin\lambda)\right], \tag{33}$$

where the dimensionless quantities are defined as

$$\begin{aligned} m_1 &= p_1 + \frac{1}{\Omega}\frac{dp_2}{dt} \\ m_2 &= p_2 - \frac{1}{\Omega}\frac{dp_1}{dt} \\ m_3 &= \frac{1}{\Omega}\frac{dp_3}{dt} \end{aligned} \tag{34}$$

The quantities p_i are related to the Earth's orientation parameters (X and Y) and length-of-day variations provided by IERS (EOPC04 series)

$$\begin{aligned} p_1 &= X \\ p_2 &= -Y \\ p_3 &= \Omega(UT1 - TAI) \end{aligned}, \tag{35}$$

where $UT1$ and TAI are the Universal Time and the International Atomic Time. Ω is the Earth's mean angular velocity.

Daily gravity changes induced by the Earth's rotation variations are interpolated to 6 hr time span and are subtracted from filtered gravity variations.

4.2 Practical computation of global atmospheric loading

The spatial sampling of the pressure fields provided by meteorological centres are respectively 2.5 and 1.125 degrees for NCEP and ECMWF. The accuracy is about 10 Pa (0.1 millibar).

The local pressure measurements, in conjunction with surface gravity, are available with a precision of about 1 Pa (0.01 millibar). As we pointed out before, the Newtonian attraction is induced by regional (about 1000 km around the station) pressure variations. We would like to use these precise local pressure measurements to enhance our computations. For this reason, we choose to separate the practical computation of global atmospheric loading as the convolution of elastic and Newtonian Green's functions with pressure into two spatial domains.

(1) a near area, called zone 1, for which the pressure is assumed to be constant and equal to the pressure measured at the gravity station. We choose to represent this area as a spherical cap of radius ψ_1.

(2) a more distant area, called zone 2, for angular distances between ψ_1 and ψ_2 (ψ_2 equal to 180° corresponds to an integration on the whole Earth surface) for which we use the pressure fields provided by the meteorological centres.

Before testing the different hypotheses of Newtonian attraction (surface or pseudo-stratified models) and oceanic response to pressure forcing, i.e. inverted barometer (IB) or non-inverted barometer (NIB) hypotheses, we determine the optimal value of ψ_1, the angular radius of zone 1, which minimizes the standard deviation of surface gravity residuals.

An implicit assumption made throughout this paper is that the models leading to the smaller gravity residuals are better than those yielding larger residuals; however one has to keep in mind that other processes than atmospheric loading are affecting the data and this might modify our conclusions from the minimum variance approach.

Fig. 6 shows the standard deviation of surface gravity residuals as a function of ψ_1 for the gravimeter CO26 installed in Strasbourg (France). In the computation of atmospheric loading, we consider the local pressure measurements for angular distances between 0° and ψ_1, and the NCEP pressure field for angular distances between ψ_1 and 180°.

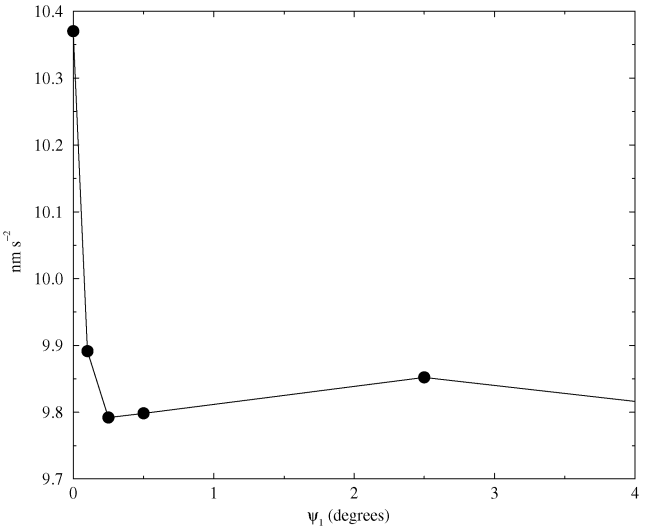

Figure 6. Determination of the optimal angular radius of homogeneous spherical cap (ψ_1) in the modelling of the local Newtonian attraction with the help of local pressure. Here ψ_2 is equal to 180°.

The value of ψ_1 equal to 0° corresponds to the use of only global pressure charts and no local pressure measurements. The optimal value of ψ_1, corresponding to a minimum in the surface gravity variance, is obtained for values between 0.25° and 0.5°. We fix henceforth the value of ψ_1 at 0.5° (about 50 km) even if we found that this value depends slightly on the site (coastal or inland).

In the next sections, we determine with the same criterion the optimal model of atmospheric loading in terms of Newtonian attraction (thin-layer or pseudo-stratified models) and oceanic response to pressure forcing (IB or NIB).

5 DETERMINATION OF THE OPTIMAL LOADING MODEL

5.1 Direct Newtonian attraction

5.1.1 Thin-layer versus pseudo-stratified model

In Section 3, we presented two different hypotheses for the operational computation of the direct Newtonian attraction: superficial thin-layer and pseudo-stratified models. We show, in this section, the differences between both hypotheses in terms of reduction of the variance of gravity residuals for SG C026, installed in Strasbourg (France).

Fig. 7 shows the decrease of the standard deviation of gravity residuals as a function of ψ_2, the angular radius of zone 2 for which we consider both hypotheses of direct Newtonian attraction. The surface pressure data are provided by NCEP. For ψ_2 equal to 0.5°, the convolution domain is restricted to zone 1. When ψ_2 is equal to 180°, the convolution domain covers the whole Earth's surface.

We also show the value of the standard deviation of gravity residues using the classical and empirical pressure correction with the help of the barometric admittance (found equal to -2.71 ± 0.03 nm s^{-2} hPa^{-1}). A thin-layer surface Newtonian model does not allow a reduction of gravity residual standard deviation versus

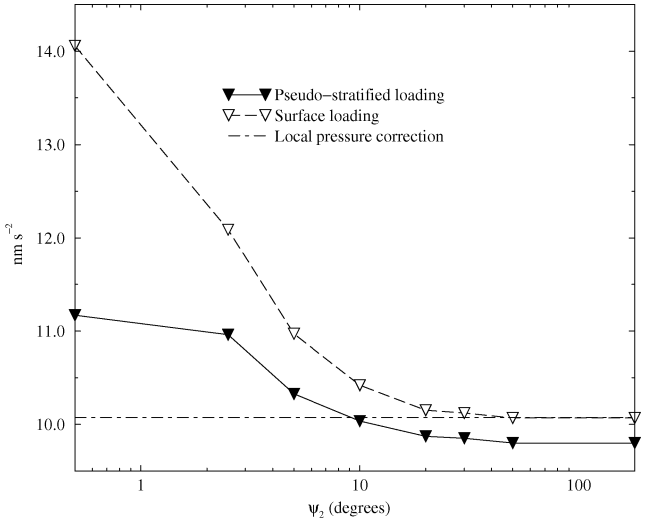

Figure 7. Reduction of the standard deviation of gravity residuals (SG C026) as a function of the solid angle ψ_2 in the integration of global pressure loading (NCEP data and IB ocean) for a surface and a pseudo-stratified processes. The value of the standard deviation of gravity residues using a local pressure correction (the admittance is equal to -2.71 ± 0.03 nm s^{-2} hPa^{-1}) is shown by the dot-dashed line.

the local empirical estimation. However, differences between pseudo-stratified and thin-layer surface attraction models become small for angular distances larger than 10°. The contribution of the pseudo-stratified model to the estimation of the direct Newtonian attraction takes into account the geometry of the atmosphere with the local horizon of the gravimeter (e.g. Merriam 1992). In fact, the atmospheric thickness is not negligible for small angular distances in the estimation of the direct Newtonian attraction.

The two curves in Fig. 7 can be decomposed into two areas. First a rapid decrease of the standard deviation between 0.5° (about 50 km) and 10.0° (about 1000 km); second a slighter decrease from 10.0° to 180.0° (i.e. by considering the pressure on the whole surface). In the first part, we model the direct Newtonian attraction increasingly better (i.e. about 90 per cent of the total signal of loading) which is induced by the regional pressure variations (i.e. about 1000 km around the gravimeter). In the second part, we estimate the elastic contribution increasingly better which is induced by large scale (wavelength larger than 4000 km) pressure variations and leads to about 10 per cent of the loading effects.

5.1.2 Effects induced by the topography around the gravimeter

In the case of SG C024, installed at TMGO (Table Mountain Geodetic Observatory), near the Rocky Mountains close to Boulder (Colorado), we cannot neglect topography in the computation of atmospheric loading. Fig. 8 shows the topography around.

For a gravimeter at altitude h and in (θ, λ), the Newtonian attraction Green's function is after eq. 3 equal to

$$GS_{\text{topo}}(\psi, z, h) = G\frac{(a+h)-(a+z)\cos\psi}{((a+z)^2+(a+h)^2-2(a+h)(a+z)\cos\psi)^{3/2}}. \quad (36)$$

The topography modifies the relative position of air masses compared to the local horizon. The horizon is also shifted by the value of the altitude of the gravimeter.

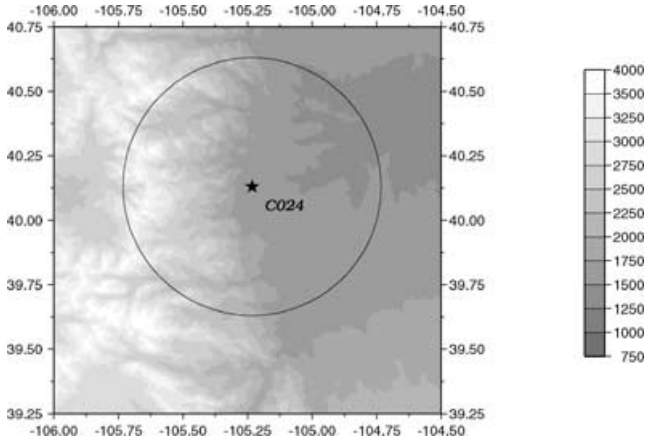

Figure 8. Topography (in m) around the station of Table Mountain (Boulder, Colorado) (latitude and longitude are expressed in degrees). The circle represents zone 1 where the pressure is assumed to be constant.

Fig. 9 shows the standard deviation of surface gravity residuals at Boulder for two global pressure loading models. The first takes into account the topography and the second does not. For both models, the oceans are supposed to respond like an IB process and the Newtonian attraction is modelled using the pseudo-stratified model.

Fig. 9 demonstrates that the topography must be taken into account in the computation of the Newtonian attraction in this case. For large distances ($\psi_2 > 10°$), the differences between both models become small, showing once more that the Newtonian attraction is a regional (about 1000 km around the station) process.

5.2 Effects due to differences between NCEP and ECMWF surface pressure fields

For SG T005, the previous instrument in Strasbourg (1987–1996), we have corrected gravity measurements with two global surface pressure data sets provided by ECMWF and NCEP. Since the

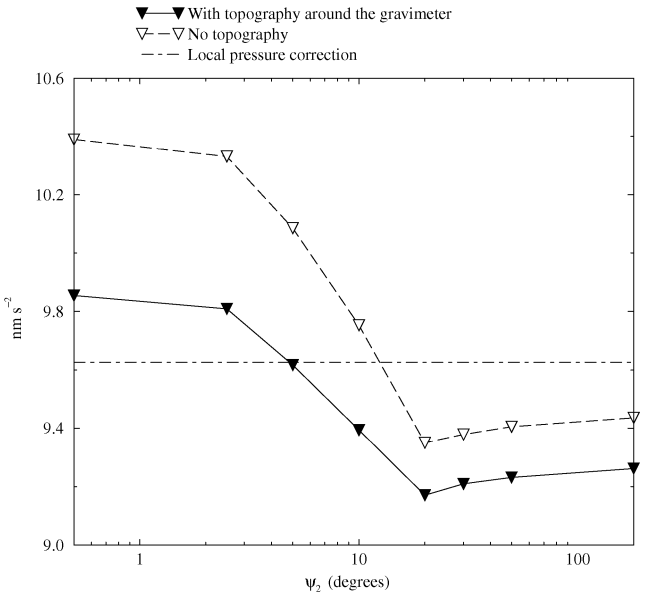

Figure 9. Reduction of the standard deviation of gravity residuals (SG C024) as a function of the solid angle ψ_2 in the integration of global pressure loading (NCEP data, pseudo-stratified model and IB ocean) by taking or not into account the topography around the station at Boulder (Colorado).

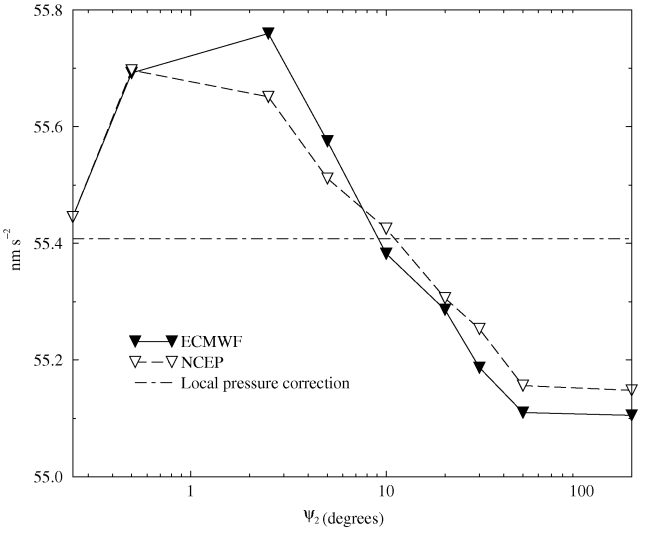

Figure 10. Reduction of the standard deviation of gravity residuals as a function of the solid angle ψ_2 in the integration of global pressure loading (pseudo-stratified model) in Strasbourg (SG T005) with pressure charts provided by ECMWF and NCEP. The standard deviation of gravity residuals with the local barometric admittance correction is shown by the dot-dashed line.

ECMWF pressure data were not available to us for the period 1997–2000 when SG CO26 was in operation in Strasbourg, we selected the 1987–1996 series of former SG T005 to test the differences between NCEP and ECMWF pressure fields.

Fig. 10 shows the reduction of the standard deviation of gravity residuals as a function of the solid angle ψ_2 in the integration of atmospheric loading (pseudo-stratified model). The ocean is modelled as responding to pressure forcing with the IB approximation. ECMWF versus NCEP pressure data allow a greater reduction of gravity residuals. This is partly due to the spatial sampling of ECMWF charts (1.125° versus 2.5° for NCEP) that allows a better estimation of regional high frequency pressure variations.

One can notice that the reduction of the gravity residual standard deviation leads to a level (about 10 nm s^{-2}, as shown by Fig. 7) in the new series (CO26) which is approximately five times lower than for the older series (T005). This is because of a higher noise level (instrumental + acquisition system) in the previous instrument (Boy *et al.* 2000).

We have demonstrated in this section that the thin-layer surface approach is not adequate for reducing the variance of gravity residuals, compared to the local estimate using the barometric admittance correction. The simplified computation of the direct Newtonian attraction using the pseudo-stratified model, which approximates atmospheric density variations with height using only surface pressure data, allows a significant reduction of the standard deviation of surface gravity residuals of about 20 per cent (Fig. 7) over the whole spectral domain (from 12 hr to 2 yr) compared to usual local pressure approach.

In the case of high topographic variations around the gravimeter (here the case of Boulder, Colorado), we need to take them into account in the computation of the direct Newtonian attraction. The reduction of the standard deviation of surface gravity residuals is about 2 per cent for SG C024 (Boulder) compared to the case of neglecting the topography. For others SGs, we cannot observe a significant reduction of the gravity residual variance by taking into account the topography around the stations.

5.3 Oceanic response to pressure forcing

5.3.1 Inverted and non-inverted barometer approximations

The oceanic response to pressure is classically modelled by two different assumptions:

(1) the non-inverted barometer (NIB). Atmospheric pressure variations are fully transmitted to the sea floor and the oceanic response is the same as for the solid Earth. The convolution domain is hence the whole Earth surface.

(2) the inverted barometer (IB). Pressure variations δp_A are compensated by static variations of sea height δh_w. There is no net pressure variation on the sea floor (Dickman 1988),

$$\delta h_w = -\frac{\delta p_A}{\rho_w g_0}, \tag{37}$$

where ρ_w is the mean water density. In this case, the convolution of the pressure field with Green's functions (elastic and Newtonian parts) is restricted to the continents.

In Boy *et al.* (1998), a non-global static ocean response to air pressure changes was favoured. We only consider here the classical IB and NIB hypotheses for the ocean response as a more recent estimate leads to almost no significant changes between IB and the static ocean response (even for low harmonic degrees).

We use the ocean–continent function with a spatial sampling of 0.5° (about 50 km), smaller than the global atmospheric data sampling, defined as follows

$$O(\theta, \lambda) = \begin{cases} 0 \text{ if } (\theta, \lambda) \in \text{oceans} \\ 1 \text{ if } (\theta, \lambda) \in \text{continents} \end{cases}. \tag{38}$$

This sampling allows an accurate estimation of the coastal geometry, which is important in the loading computation for stations close to the sea.

5.3.2 Oceanic response to pressure forcing observed by SGs

We study the oceanic response to pressure forcing with the six SG data sets exploring the variations of standard deviation of surface gravity residuals with ψ_2, the angular radius of the convolution domain, under the IB and NIB hypotheses described above.

Fig. 11 shows the reduction of the standard deviation of gravity residuals of the six SGs as a function of ψ_2 (NCEP and pseudo-stratified model) for both hypotheses of oceanic response (IB and NIB) to pressure forcing. In general, the loading model which integrates over the whole Earth ($\psi_2 = 180°$) with the IB hypothesis allows a reduction in the standard deviation of gravity residuals compared to the local empirical admittance correction. For Membach (Belgium), the lowest standard deviation is obtained with the local pressure correction; this fact might be due to non-static ocean loading effects near the North and Baltic Seas.

For all SGs, the standard deviation of gravity residuals is larger with the NIB hypothesis than with the IB assumption, except for Boulder where there is no significant discrepancy.

For SGs close to the sea (Canberra and Esashi), differences between IB and NIB hypotheses become large because gravity variations are sensitive to local Newtonian attraction of both ocean and atmosphere. For SGs far from coasts (Boulder and Vienna), the oceanic effect on gravity is mainly due to large scale elastic deformation which is smaller than the direct attraction.

In fact, for SGs in the vicinity of oceans, typically for distances smaller than 1000 km, the Newtonian attraction of the

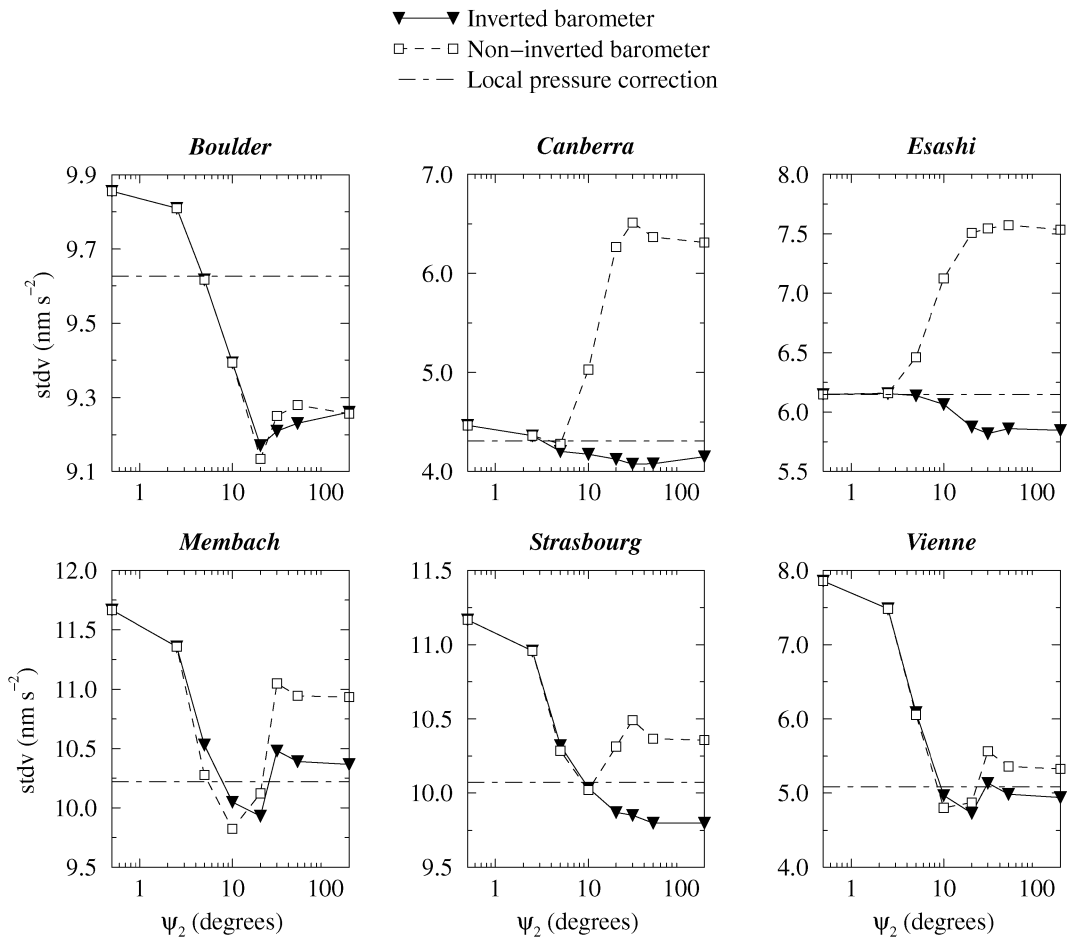

Figure 11. Reduction of the standard deviation of gravity residuals as a function of the solid angle ψ_2 in the integration of global pressure loading (NCEP data and pseudo-stratified model) for IB (triangles and solid lines) and NIB (squares and dashed lines) oceans. The standard deviation of gravity residuals with the local barometric admittance correction is shown by dot-dashed lines.

oceans is not negligible and we have to take into account the dynamical response of oceans to pressure forcing (Dickman 1998); for periods shorter than ten days, this dynamical response differs considerably from a static response (Wunsch & Stammer 1997).

5.4 Consequences in the spectral domain

We now demonstrate that the pseudo-stratified approximation for the computation of the direct Newtonian attraction plus the IB hypothesis of the oceanic response lead to the optimal model for estimating global atmospheric loading effects on surface gravity. Fig. 12 shows the spectrum of surface gravity residuals for SG C026 (Strasbourg, France) before any atmospheric correction, and with local and global atmospheric corrections.

The global atmospheric loading, modelled with the help of global pressure charts (NCEP), allows a significant reduction of gravity residuals for periods between about 5 and 100 days versus a local pressure estimate for SG CO26 (Strasbourg). For longer periods, the atmosphere does not seem to be the major source of surface gravity perturbations at Strasbourg, especially for seasonal and annual period ranges. We do not model other environmental contributions such as oceanic circulation or soil moisture which can lead in some cases to effects reaching several tens of nm s^{-2} (Van Dam & Wahr 1998).

The results are very similar for others SGs, i.e. the global atmospheric loading modelling allows a systematic and significant reduction of gravity residuals versus the classical local estimation using barometric admittance. However the frequency range of this reduction depends on the locations of the SG. For SGs away from the sea (Boulder and Vienna), the short period limit is about a couple of days whereas for SGs close to the sea (Canberra, Esashi and Membach), this limit increases to about 10 days. It proves that the oceans are, besides the atmosphere, one of the major sources of surface gravity perturbations which are not yet well modelled . The long-period limit also varies considerably according to the location of the station.

We show in Fig. 13 the spectral amplitudes of the gravity residues according to both NIB and IB hypotheses for the Strasbourg station; the level is significantly lower for periods between 5 and 100 days. This fact is also true for most of the other SG stations. For shorter periods, the ocean response to pressure is no longer static as shown by Wunsch & Stammer (1997).

6 CONCLUSION

We have demonstrated that the optimal model of computation of the loading of a global atmospheric model includes a pseudo-stratified atmosphere for the direct Newtonian attraction and the inverted barometer for the response of oceans to pressure forcing. The

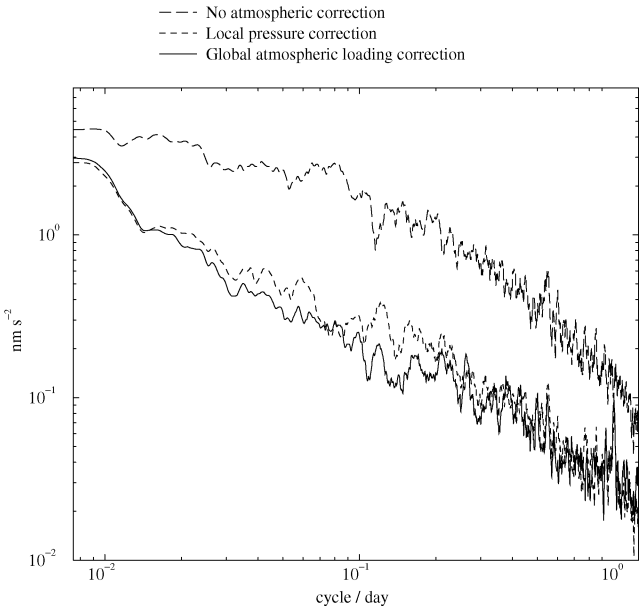

Figure 12. Gravity residuals after Earth tidal analysis of SG C026 (Strasbourg, France) data with two different pressure corrections: a local pressure correction (with an admittance equal to -2.71 ± 0.03 nm s^{-2} hPa^{-1}) and global pressure loading (pseudo-stratified model) with $\psi_1 = 0.5^\circ$ and $\psi_2 = 180^\circ$ and using NCEP pressure charts. The oceanic response to pressure forcing is modelled using IB hypothesis.

pseudo-stratified model takes into account the atmospheric thickness, which is not negligible, and allows a simplified convolution of surface pressure field with Green's functions compared to the complete 3-D atmosphere.

We have also shown that the non-inverted barometer is definitively not an adequate assumption for describing the oceanic response to pressure forcing.

The oceans are also one of the major sources of surface gravity perturbations which are not until now well-modelled. The next step is to estimate oceanic loading effects on gravity using, for example, altimetric data provided by Topex–Poseidon or global circulation models.

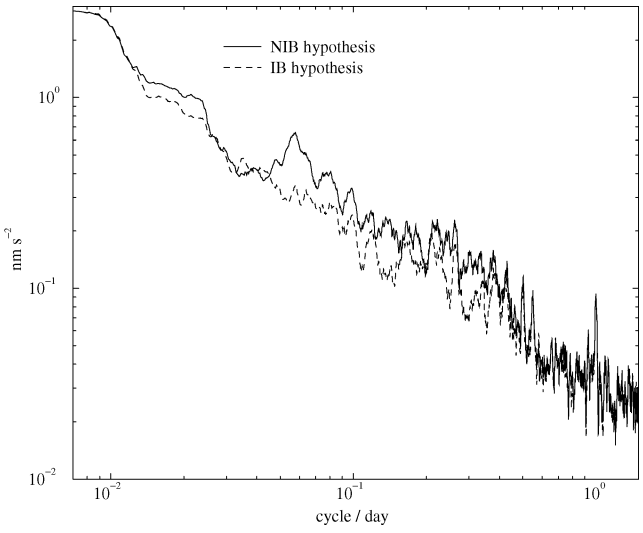

Figure 13. Gravity residuals after Earth tidal analysis of SG C026 (Strasbourg, France) data and global pressure corrections ($\psi_2 = 180^\circ$) with both NIB (solid line) and IB (dashed line) assumptions.

ACKNOWLEDGMENTS

We acknowledge GGP members for providing gravity/pressure data and the data bank (etggp) located at ICET (International Centre of Earth Tides) at Brussels (Belgium). We are also grateful to the National Center for Environmental Prediction (NCEP) and the European Centre of Medium-Range Weather Forecasts (ECMWF) for having kindly provided the pressure data on which this study is based. We tank S. Dickman and an anonymous referee for their comments and suggestions that helped in improving the manuscript.

REFERENCES

Boy, J.P., 2000. Effets des surcharges atmosphériques sur les variations de gravité et les déplacements de surface de la Terre, *PhD Thesis,* Université Louis Pasteur, Strasbourg, France.

Boy, J.P., Hinderer, J. & Gegout, P., 1998. Global atmospheric loading and gravity, *Phys. Earth planet. Inter.,* **109,** 161–177.

Boy, J.P., Hinderer, J., Amalvict, M. & Calais, E., 2000. On the use of long records of superconducting and absolute gravity observations with special application to the Strasbourg station, France, *Cahiers du Centre Européen de Géodynamique et de Séismologie,* **17,** 67–83.

Crossley, D.J., Hinderer, J., Jensen, O.G. & Xu, H., 1993. A slew rate detection criterion applied to SG data processing, *Bull. Inf. Marees Terr.,* **117,** 8675–8704.

Crossley, D.J., Jensen, O.G. & Hinderer, J., 1995. Effective barometric admittance and gravity residuals, *Phys. Earth planet. Inter.,* **90,** 221–241.

Crossley, D.J. *et al.*, 1999. Network of superconducting gravimeters benefits a number of disciplines, *EOS, Trans. Am. geophys. Un.,* **80,** 121–126.

Dickman, S.R., 1988. Theoretical investigation of the oceanic inverted barometer response, *J. geophys. Res.,* **93,** 14 941–14 946.

Dickman, S.R., 1998. Determination of oceanic dynamic barometer corrections to atmospheric excitation of Earth rotation, *J. geophys. Res.,* **103,** 15 127–15 143.

Dziewonski, A.M. & Anderson, D.L., 1981. Preliminary Reference Earth Model, *Phys. Earth planet. Inter.,* **25,** 297–356.

ECMWF, 1994. The description of ECMWF/WCRP Level III-A Global Atmospheric Data.

Farrell, W.E., 1972. Deformation of the Earth by surface loads, *Rev. geophys. Space Phys.,* **10,** 761–797.

Francis, O. & Dehant, V., 1985. Recomputation of the Green's functions for tidal loading estimations, *Bull. Inf. Marees Terr.,* **100,** 6962–6986.

Gill, A.E., 1982. *Atmosphere–Ocean Dynamics,* Academic Press, New York.

Green, J., 1999. *Atmospheric Dynamics,* Cambridge University Press, Cambridge.

Greff-Lefftz, M. & Legros, H., 1997. Some remarks about the degree one deformations of the Earth, *Geophys. J. Int.,* **131,** 699–723.

Hinderer, J. & Legros, H., 1989. Elasto-gravitational deformation, relative gravity changes and Earth dynamics, *Geophys. J. Int.,* **97,** 481–495.

Loyer, S., Hinderer, J. & Boy, J.P., 1999. Determination of the gravimetric factor at Chandler period from Earth's orientation data and superconducting gravimetry observations, *Geophys. J. Int.,* **136,** 1–7.

Merriam, J.B., 1992. Atmospheric pressure and gravity, *Geophys. J. Int.,* **109,** 488–500.

Mukai, A., Higashi, T., Takemoto, S., Nakagawa, I. & Naito, I., 1995. Accurate estimation of atmospheric effects on gravity observations made with a superconducting gravity meter at Kyoto, *Phys. Earth planet. Inter.,* **91,** 149–159.

NOAA/NASA/USAF, 1976. *U.S. Standard Atmosphere 1976,* Washington, DC.

Sneeuw, N. & Bun, R., 1996. Global spherical harmonic computation by two-dimensional Fourier methods, *J. Geodesy,* **70,** 224–232.

Spratt, R.S., 1982. Modelling the effect of atmospheric pressure variations on gravity, *Geophys. J. R. astr. Soc.,* **71,** 173–186.

Van Dam, T.M. & Wahr, J., 1998. Modeling environment loading effects: a review, *Phys. chem. Earth,* **23,** 1077–1087.

Warburton, R.J. & Goodkind, J.M., 1977. The influence of barometric pressure variations on gravity, *Geophys. J. R. astr. Soc.,* **48,** 281–292.

Wenzel, H.G., 1996. The nanogal software: earth tide data processing package ETERNA 3.30, *Bull. Inf. Mar. Terr.,* **124,** 9425–9439.

Wunsch, C. & Stammer, D., 1997. Atmospheric loading and the 'inverted barometer' effect, *Rev. Geophys.,* **35,** 79–107.

Xie, L. & Dickman, S.R., 1995. North Sea pole tide dynamics, *Geophys. J. Int.,* **121,** 117–135.